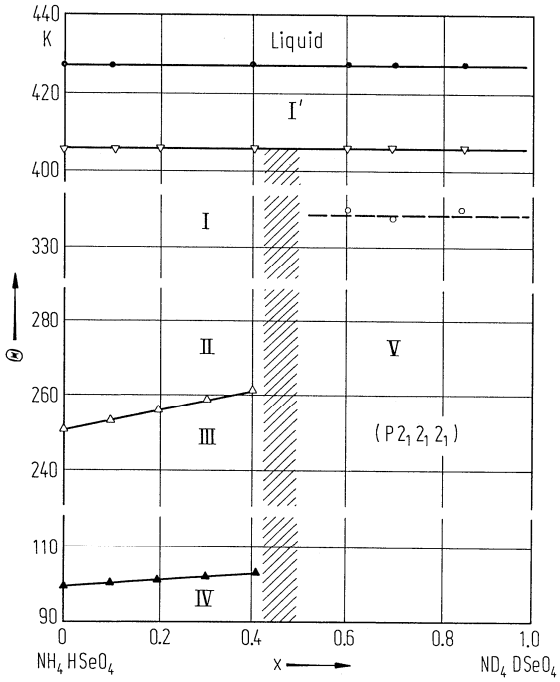

Fig. 40A-9-001. NH_4HSeO_4–ND_4DSeO_4. Θ vs. x [84Cza]. x: molar fraction of D.

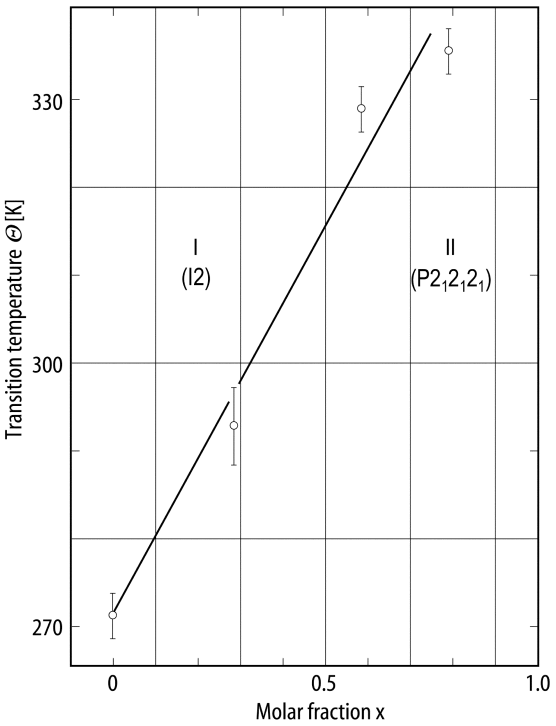

Fig. 40A-9-002. NH_4HSeO_4–ND_4DSeO_4. Θ_{II-I} vs. x [88Suk]. x: molar fraction of D.

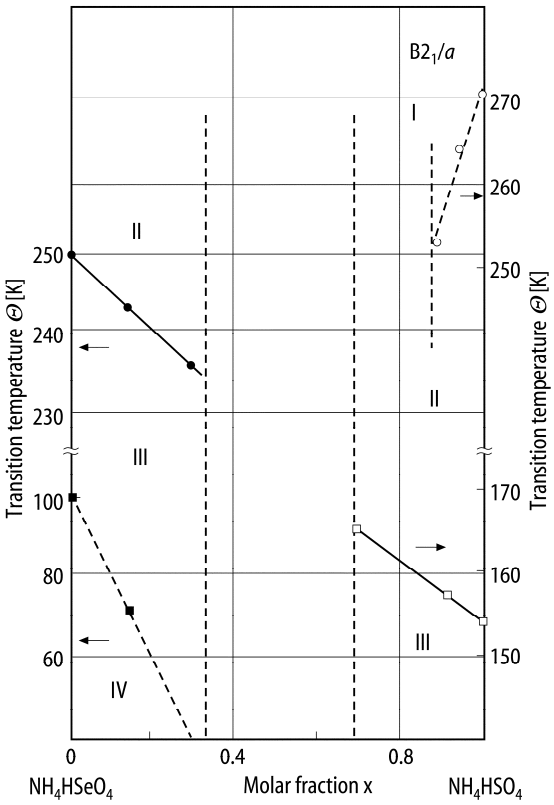

Fig. 40A-9-003. NH_4HSeO_4–NH_4HSO_4. Θ vs. x [88Mro]. x: molar fraction of SO_4.

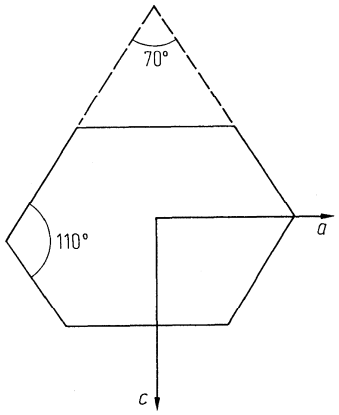

Fig. 40A-9-004. NH_4HSeO_4. Crystal form [79Cza].

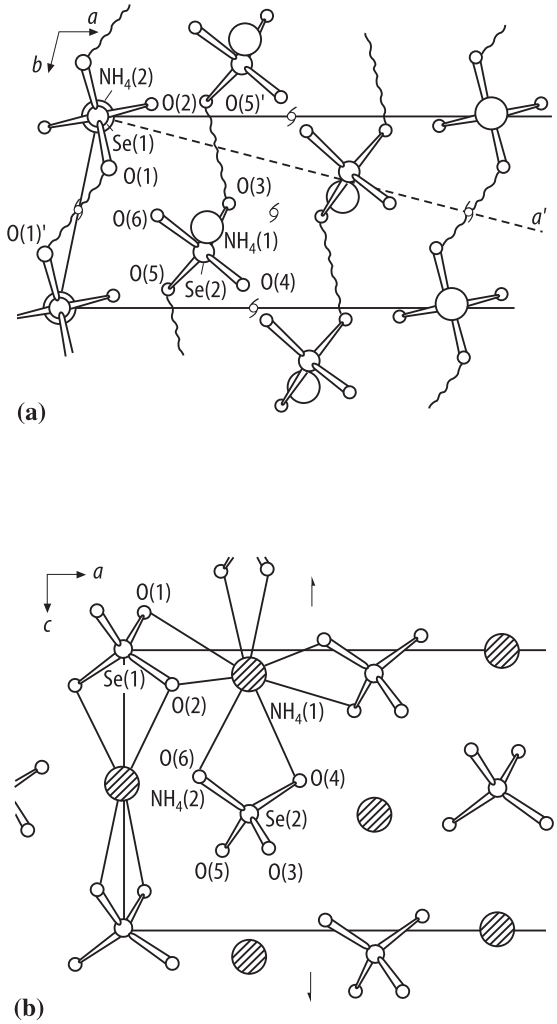

Fig. 40A-9-005. NH_4HSeO_4. Structure of phase I [80Kru]. $T = 293$ K. (**a**) Projection on the *ab* plane along the *c* axis. A half of the unit cell is shown. Wavy lines denote hydrogen bonds. The dashed line denotes the [110] direction. (**b**) Projection on the *ac* plane. The solid lines denote the bonds of the NH_4 cations with their surrounding oxygen atoms.

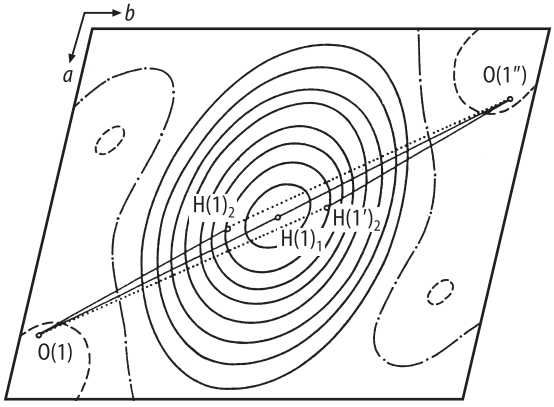

Fig. 40A-9-006. NH_4HSeO_4. Nuclear density [90Mak2]. Distribution of nuclear density of hydrogens of $N(1)H_4$ on *a*–*b* plane. $T = 400$ K.

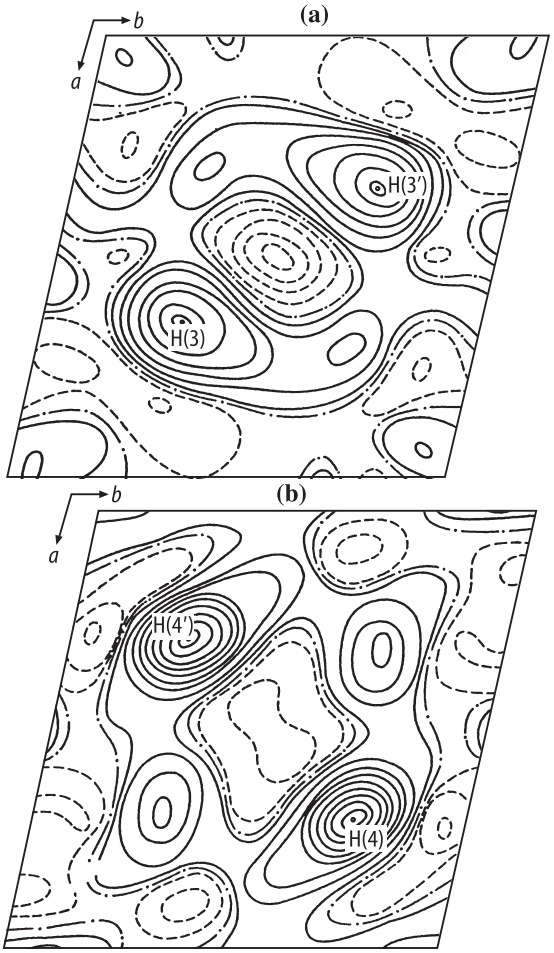

Fig. 40A-9-007. NH_4HSeO_4. Nuclear density [90Mak2]. Distribution of nuclear density of hydrogens of $N(1)H_4$ on *a*–*b* plane. $T = 293$ K.

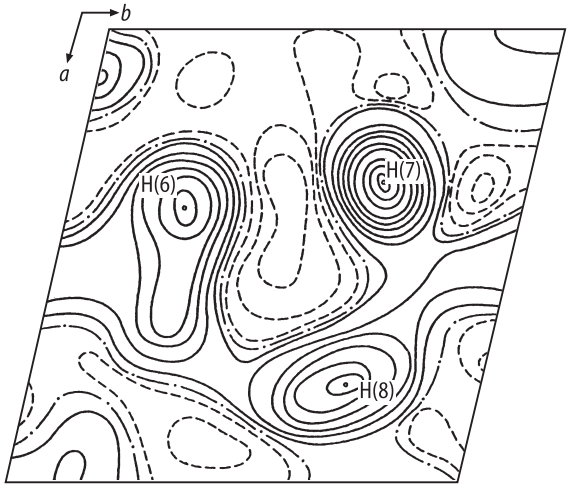

Fig. 40A-9-008. NH_4HSeO_4. Nuclear density [90Mak2]. Distribution of nuclear density of hydrogens of $N(2)H_4$ on *a*–*b* plane. $T = 293$ K.

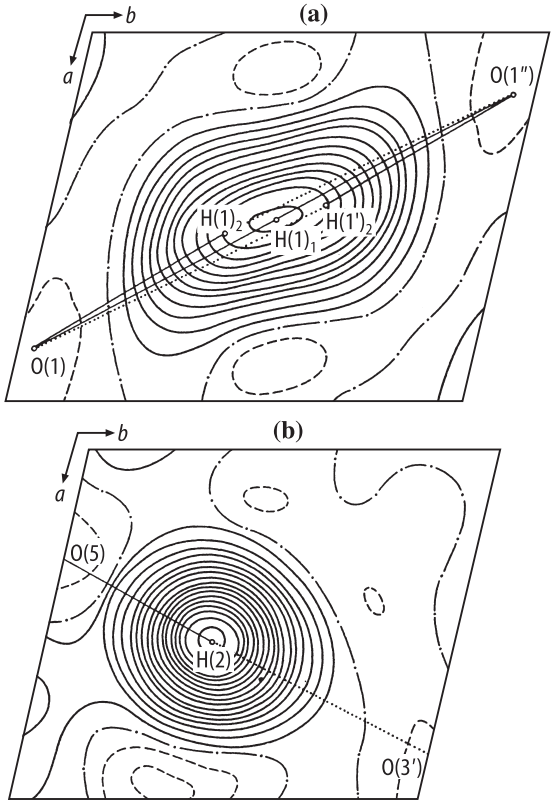

Fig. 40A-9-009. NH_4HSeO_4. Nuclear density [90Mak2]. Distribution of nuclear density of (**a**) H(1) and (**b**) H(2) on *a*–*b* plane. $T = 293$ K.

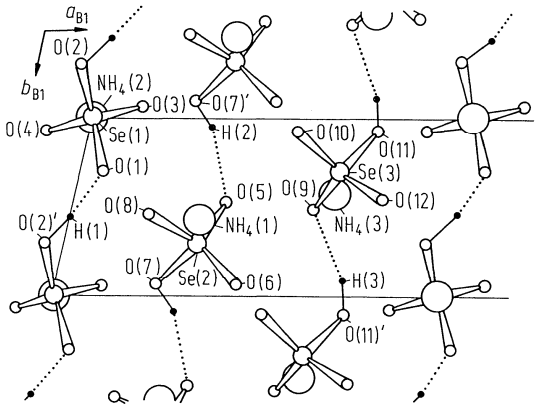

Fig. 40A-9-010. NH_4HSeO_4. Structure of phase III [80Kru]. $T = 223$ K. Projection along *c* axis. A half of the B1 cell is shown.

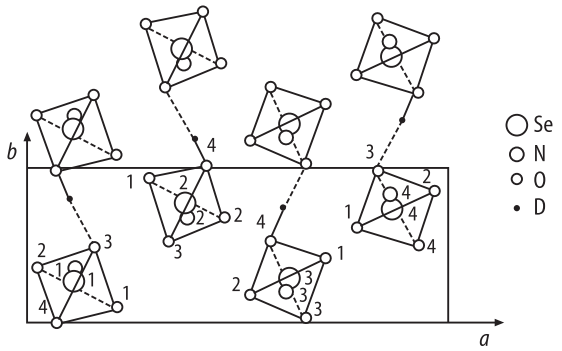

Fig. 40A-9-011. ND_4DSeO_4. Crystal structure at RT [82Was]. Projection along the *c* axis.

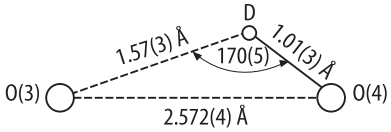

Fig. 40A-9-012. ND_4DSeO_4. Crystal structure at RT [82Was]. Interatomic distances [Å] and angles [°] of hydrogen bonds.

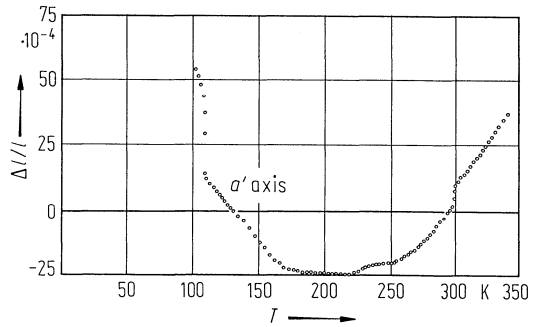

Fig. 40A-9-013. NH_4HSeO_4. $\Delta l/l$ vs. T [83Pop]. $\Delta l/l$: linear thermal expansion along the a' axis.

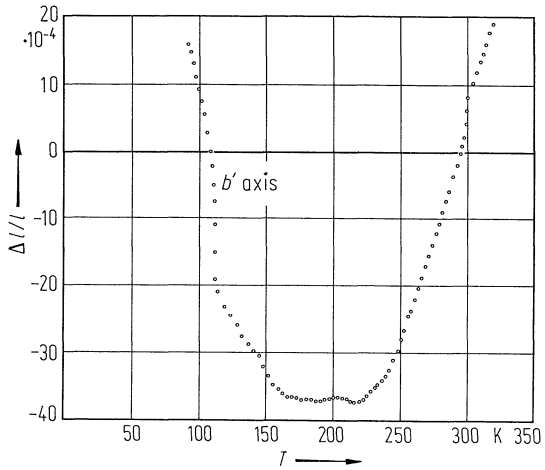

Fig. 40A-9-014. NH_4HSeO_4. $\Delta l/l$ vs. T [83Pop]. $\Delta l/l$: linear thermal expansion along the b' axis.

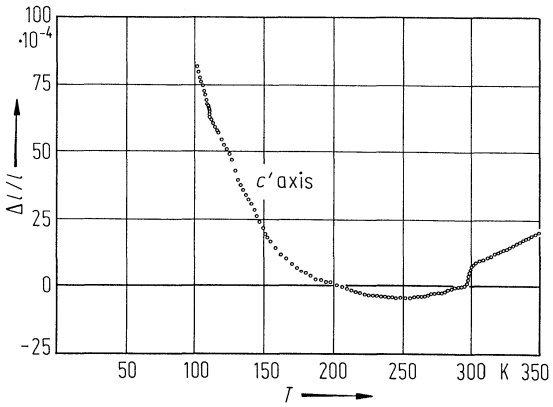

Fig. 40A-9-015. NH_4HSeO_4. $\Delta l/l$ vs. T [83Pop]. $\Delta l/l$: linear thermal expansion along the c' axis.

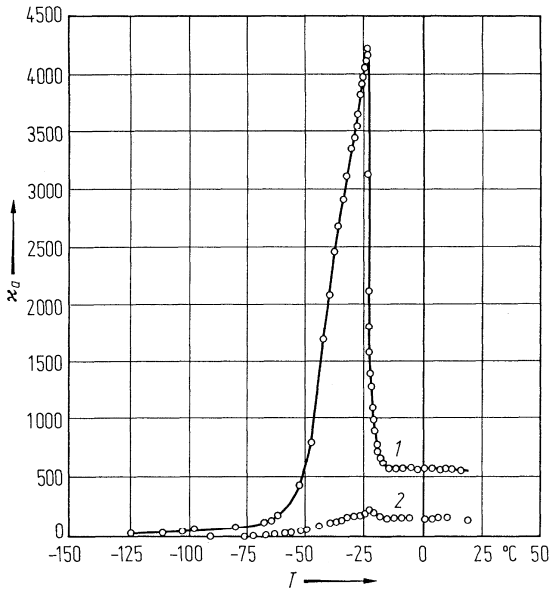

Fig. 40A-9-016. NH_4HSeO_4. κ_a vs. T [79Kra]. Curve *1*: f = 800 Hz; curve *2*: f = 10 MHz.

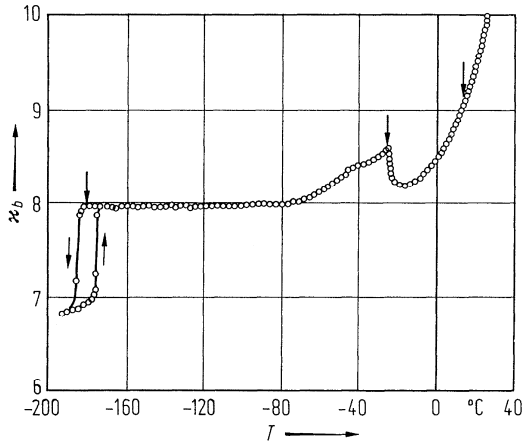

Fig. 40A-9-017. NH_4HSeO_4. $\varkappa_b$ vs. T [80Ges]. f = 1 kHz. Vertical arrows point to transition temperatures.

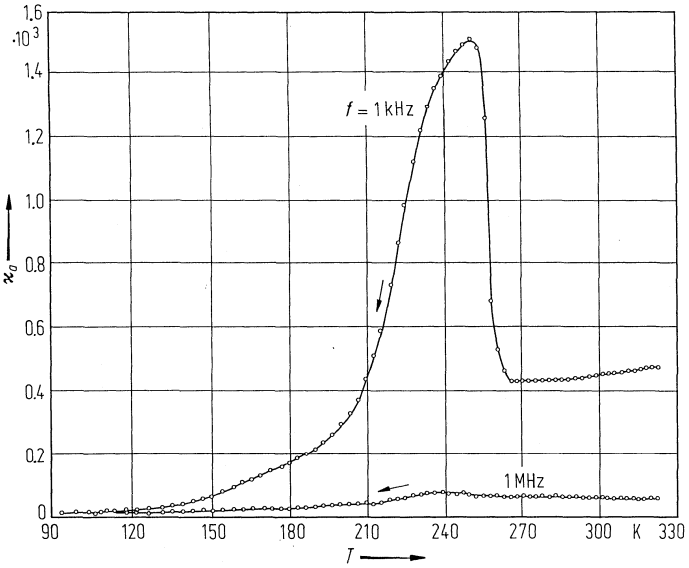

Fig. 40A-9-018. NH_4HSeO_4. $\varkappa_a$ vs. T [84Pop1]. Parameter: f.

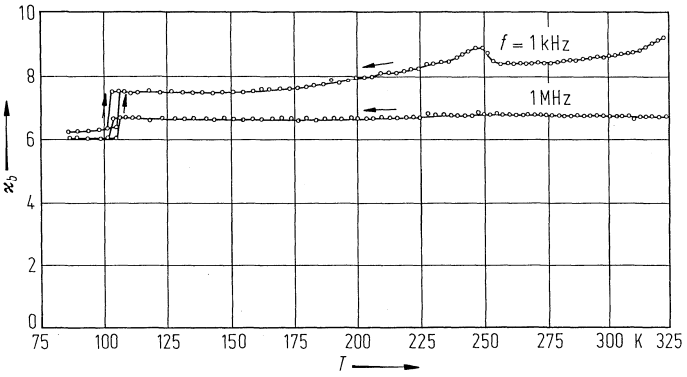

Fig. 40A-9-019. NH_4HSeO_4. $\varkappa_b$ vs. T [84Pop1]. Parameter: f.

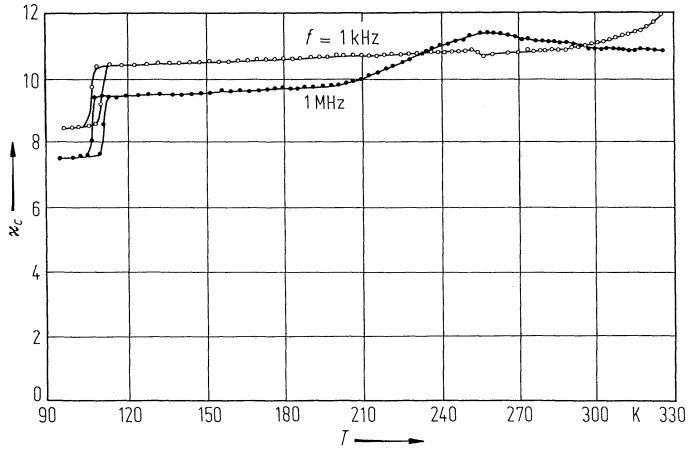

Fig. 40A-9-020. NH_4HSeO_4. κ_c vs. T [84Pop1]. Parameter: f.

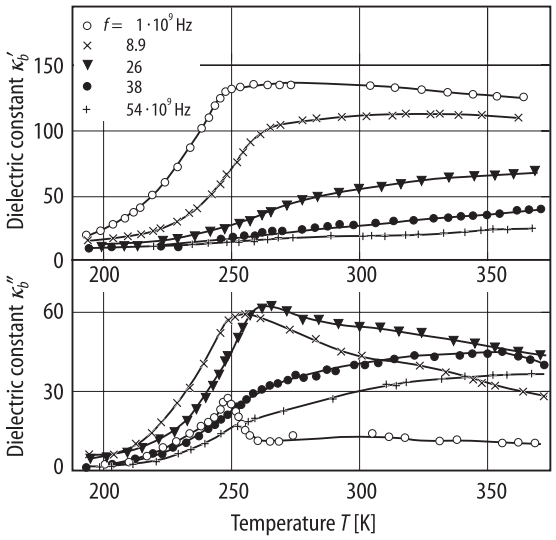

Fig. 40A-9-021. NH_4HSeO_4. κ_b', κ_b'' vs. T [95Sob]. Parameter: f.

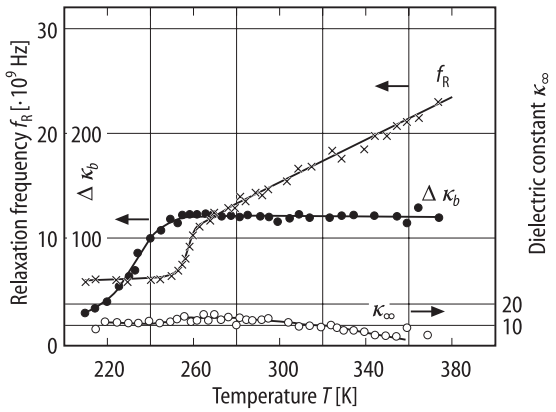

Fig. 40A-9-022. NH_4HSeO_4. $\Delta\kappa_b$, κ_∞, f_R vs. T [95Sob]. $\Delta\kappa_b = \kappa_0 - \kappa_\infty$. κ_0: static dielectric constant, f_R: relaxation frequency.

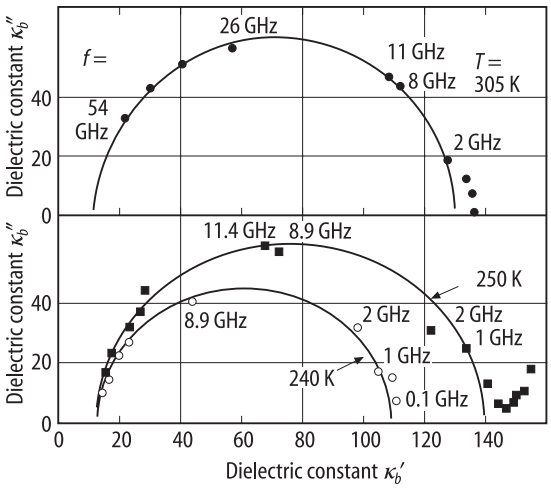

Fig. 40A-9-023. NH_4HSeO_4. Cole-Cole diagram of complex dielectric constant [95Sob]. Parameter: *T*.

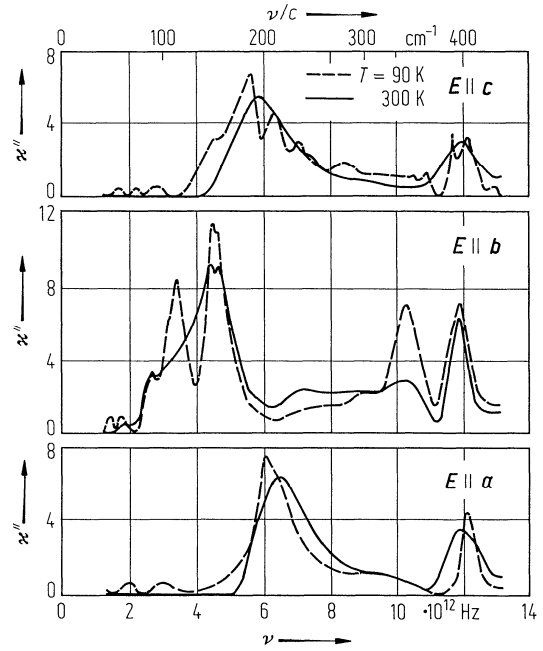

Fig. 40A-9-024. NH_4HSeO_4. κ'' vs. ν [81Kro]. The curves are obtained from reflectivity data using Kramers-Kronig relation.

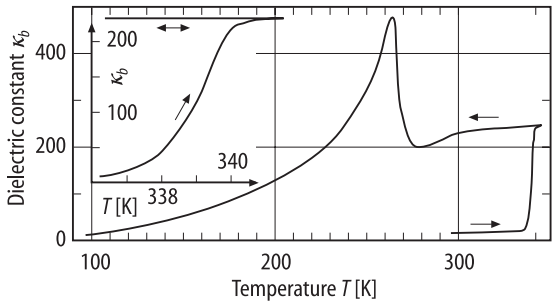

Fig. 40A-9-025. $(NH_4H)_{0.4}(ND_4D)_{0.6}SeO_4$. κ_b vs. T [87Cza].

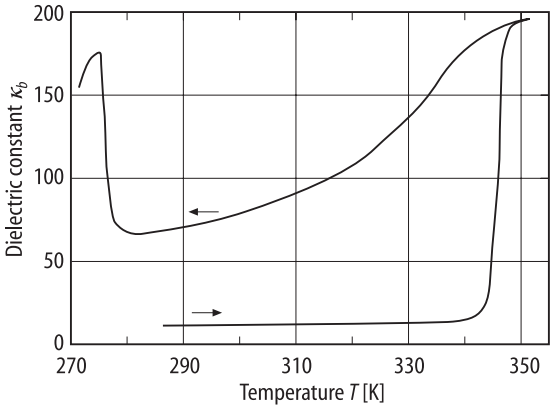

Fig. 40A-9-026. $(NH_4H)_{0.1}(ND_4D)_{0.9}SeO_4$. κ_b vs. T [87Cza].

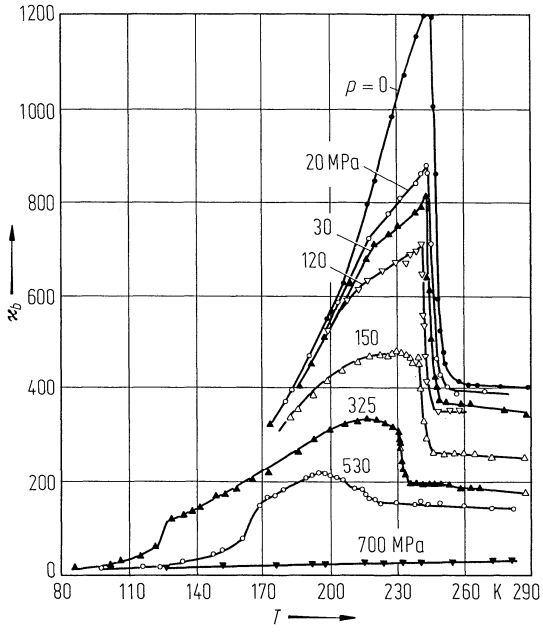

Fig. 40A-9-027. NH_4HSeO_4. κ_b vs. T [81Kra]. Parameter: p.

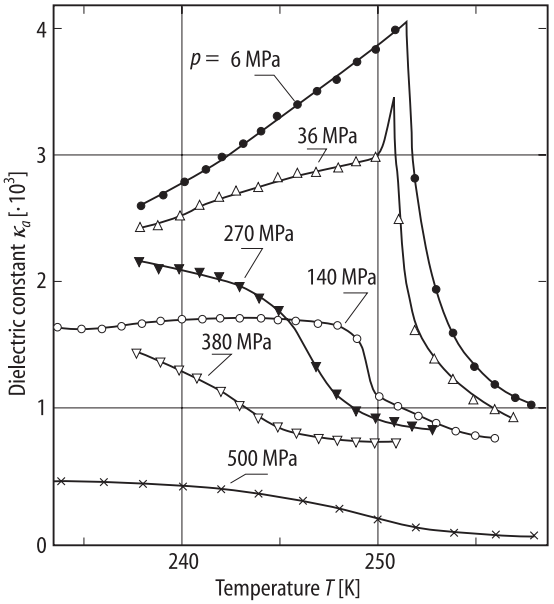

Fig. 40A-9-028. NH_4HSeO_4. κ_a vs. T [91Pop]. Parameter: p.

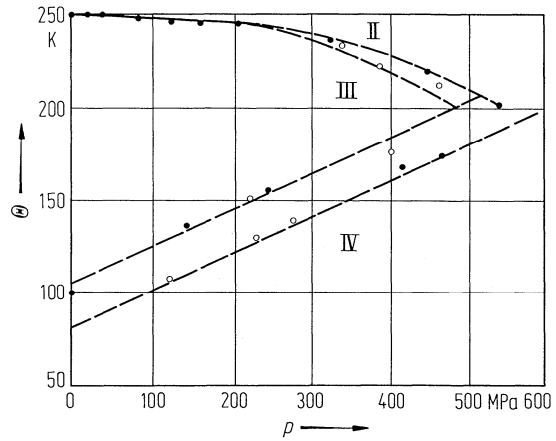

Fig. 40A-9-029. NH_4HSeO_4. Θ vs. p [81Kra]. Full circle: from measurement of κ_b; open circle: from measurement of P_s.

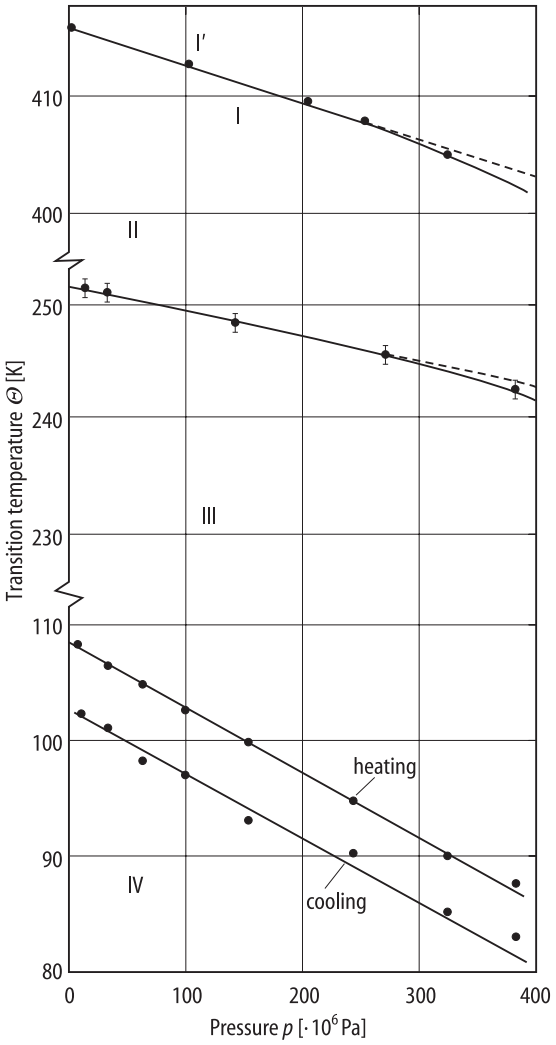

Fig. 40A-9-030. NH_4HSeO_4. Θ vs. p [91Pop].

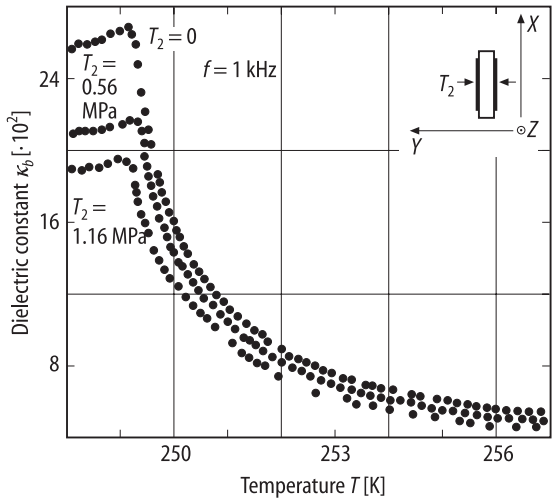

Fig. 40A-9-031. NH_4HSeO_4. κ_b vs. T [92Sty]. Parameter: T_2. T_2: compressive uniaxial stress along Y. The relation between electrodes and stress direction is shown in the insert.

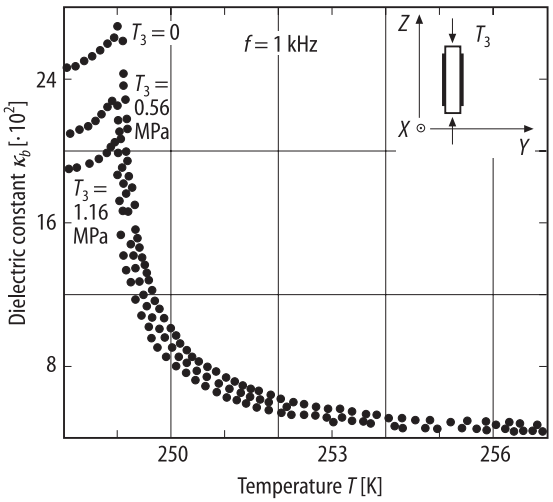

Fig. 40A-9-032. NH_4HSeO_4. κ_b vs. T [92Sty]. Parameter: T_3. T_3: compressive uniaxial stress along Z. The relation between electrodes and stress direction is shown in the insert.

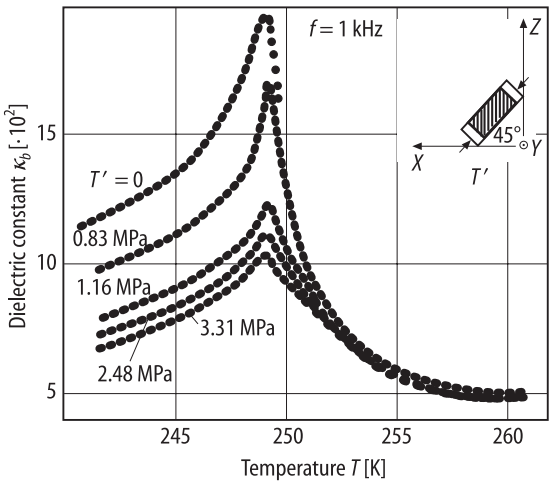

Fig. 40A-9-033. NH_4HSeO_4. κ_b vs. T [92Sty]. Parameter: T'. T': compressive uniaxial stress along the direction at 45° from $-X$ in the X–Z plane. The relation between electrodes and stress direction is shown in the insert.

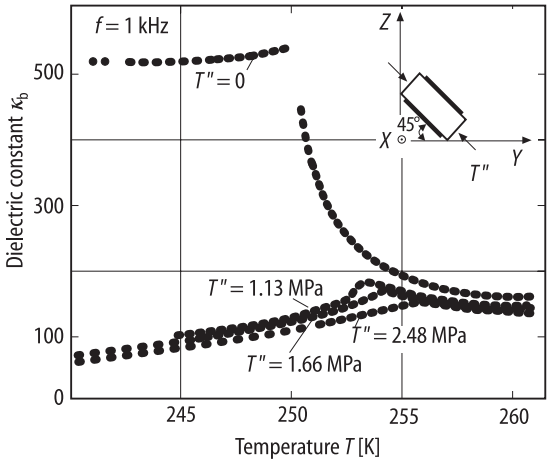

Fig. 40A-9-034. NH_4HSeO_4. κ_b vs. T [92Sty]. Parameter: T''. T'': compressive uniaxial stress along the direction at 45° from $-Y$ in the Y–Z plane. The relation between electrodes and stress direction is shown in the insert.

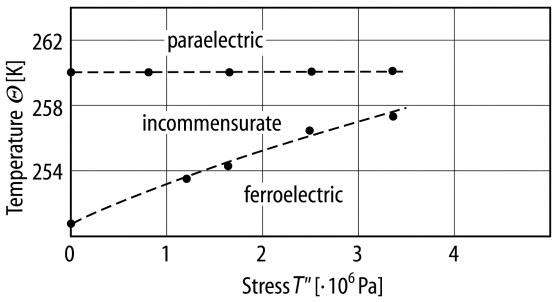

Fig. 40A-9-035. NH_4HSeO_4. Θ vs. T'' [92Sty]. T'': uniaxial compressive stress in Y–Z plane along the direction making 45° from $-Y$.

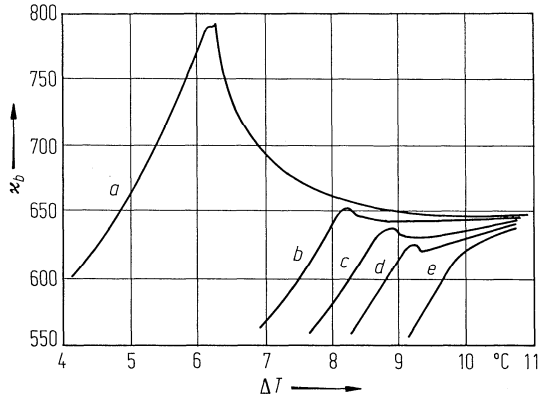

Fig. 40A-9-036. NH_4HSeO_4. κ_b vs. ΔT [87Pyk]. Parameter: E_{bias} [$\cdot 10^5$ V m^{-1}]. Curve *a*: E_{bias} = 4.63 [$\cdot 10^5$ V m^{-1}], *b*: 7.65, *c*: 8.72, *d*: 9.43, *e*: 11. $\Delta T = T - \Theta_f$. On cooling.

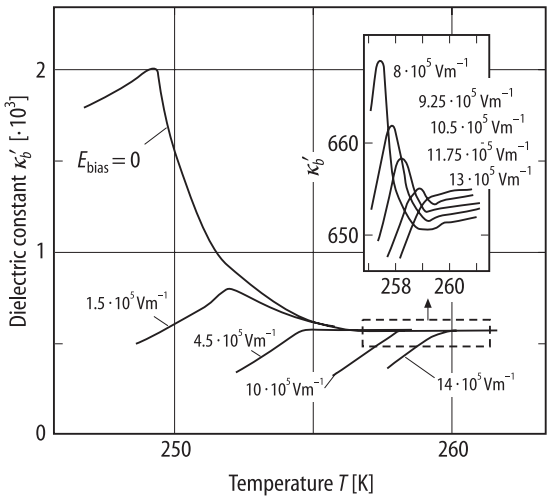

Fig. 40A-9-037. NH_4HSeO_4. κ_b' vs. T [88Kro]. Parameter: E_{bias}.

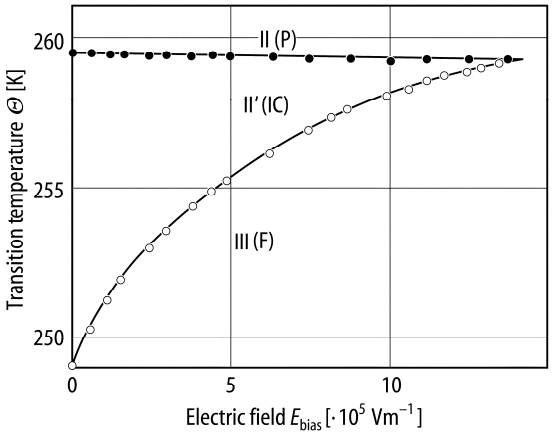

Fig. 40A-9-038. NH_4HSeO_4. Θ vs. E_{bias} [88Kro].

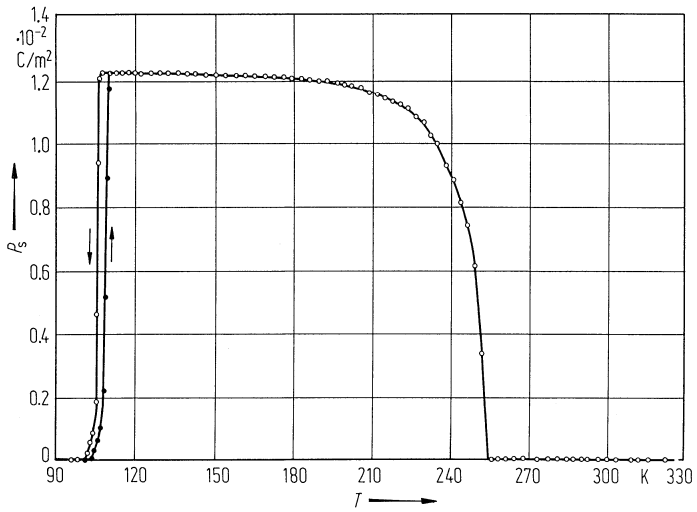

Fig. 40A-9-039. NH_4HSeO_4. P_s vs. T along the b axis [84Pop1].

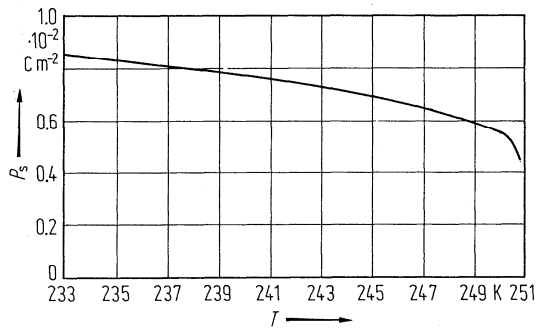

Fig. 40A-9-040. NH_4HSeO_4. P_s vs. T [80Pop].

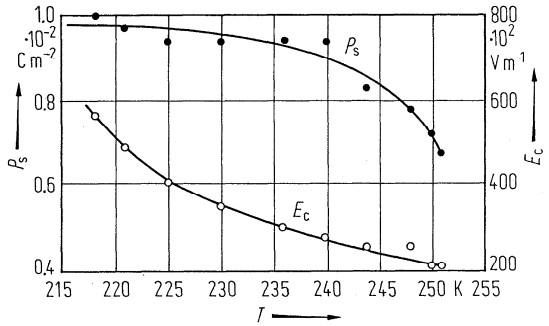

Fig. 40A-9-041. NH_4HSeO_4. P_s, E_c vs. T [79Cza].

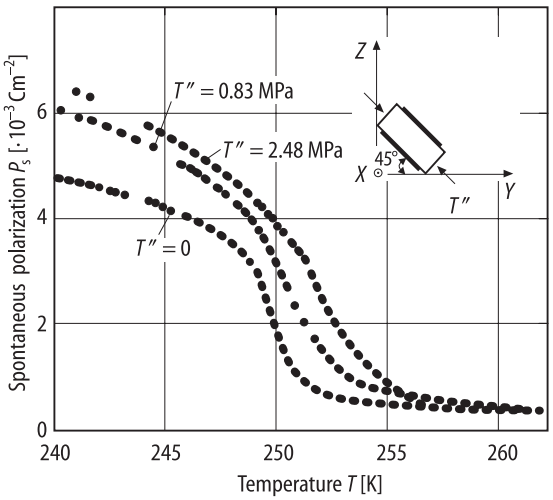

Fig. 40A-9-042. NH_4HSeO_4. P_s vs. T [92Sty]. Parameter: T''. T'': compressive uniaxial stress along the direction at 45° from $-Y$ in the Y–Z plane. The relation between electrodes and stress direction is shown in the insert.

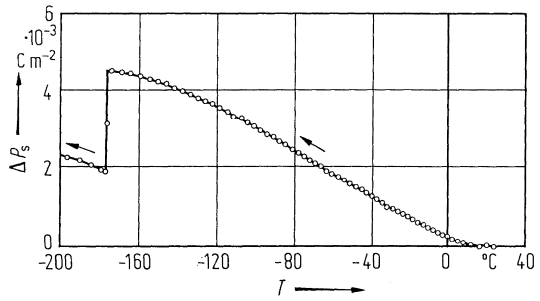

Fig. 40A-9-043. NH_4HSeO_4. ΔP_s vs. T [80Ges]. ΔP_s: pyroelectric change.

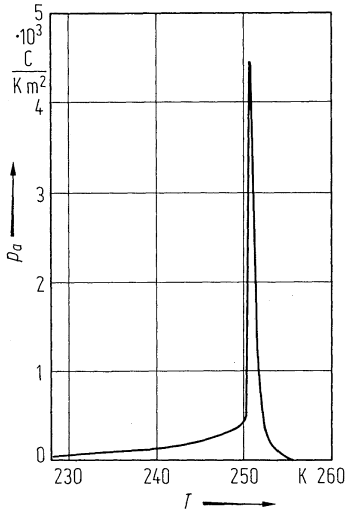

Fig. 40A-9-044. NH_4HSeO_4. p_a vs. T [80Pop]. p_a: pyroelectric coefficient along the a axis.

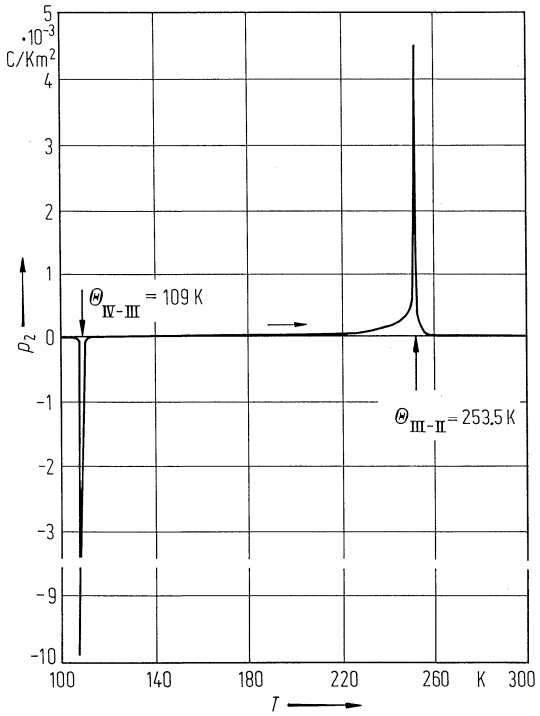

Fig. 40A-9-045. NH_4HSeO_4. p_2 vs. T [81Pop]. p_2: pyroelectric coefficient along the b axis.

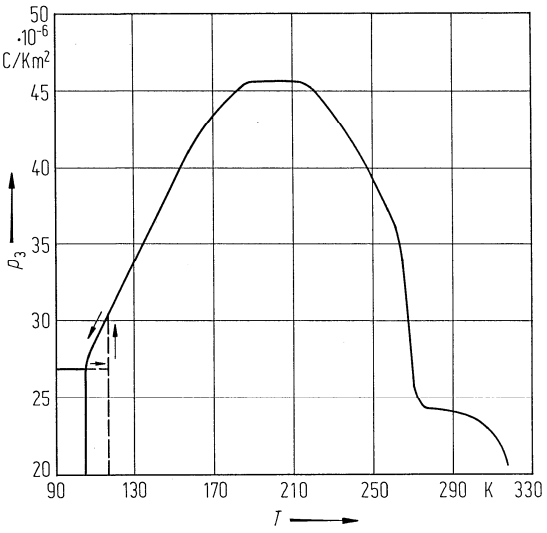

Fig. 40A-9-046. $(NH_4H)_{1-x}(ND_4D)_xSeO_4$. p_3 vs. T [86Pyk1]. x = 0.7. p_3: pyroelectric coefficient along the c axis.

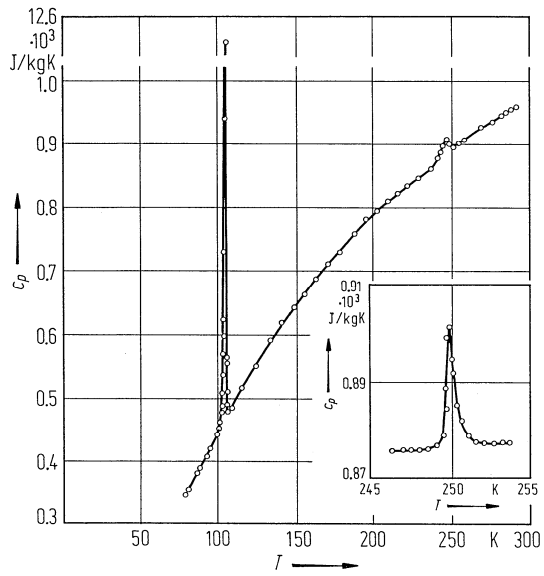

Fig. 40A-9-047. NH_4HSeO_4. c_p vs. T [84Pop2]. c_p: specific heat capacity at constant pressure.

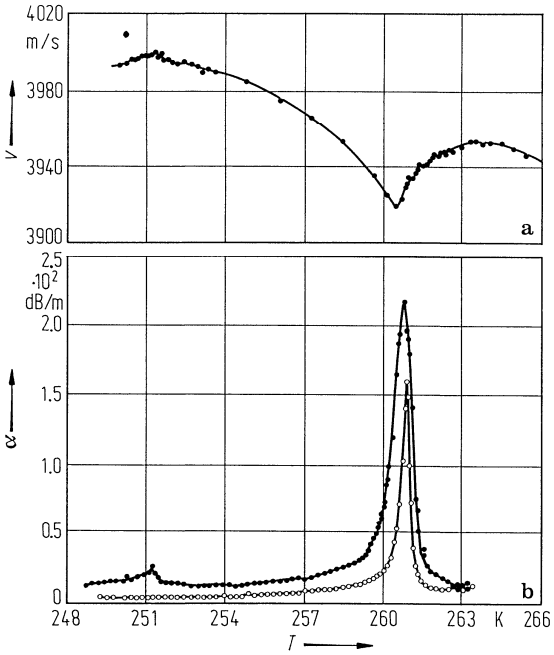

Fig. 40A-9-048. NH_4HSeO_4. (**a**) υ vs. T, (**b**) α vs. T [81Maj]. υ: longitudinal sound velocity along the b axis measured at 10 MHz. α: longitudinal sound attenuation coefficient along the b axis. Full circle: $10 \cdot 10^6$ Hz; open circle: $5 \cdot 10^6$ Hz.

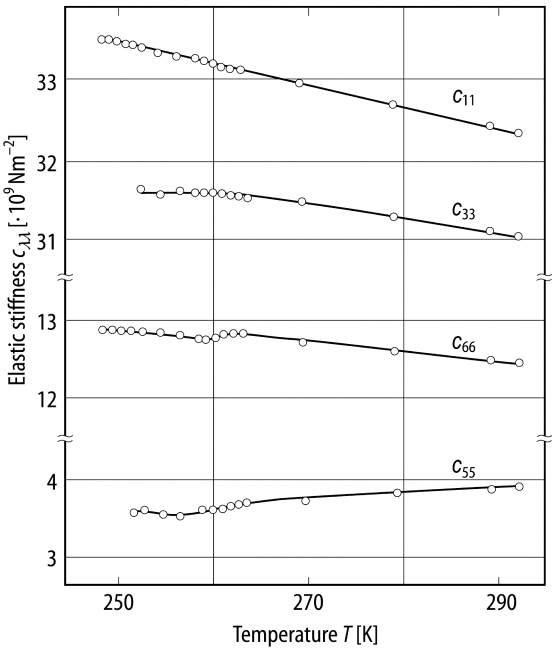

Fig. 40A-9-049. NH_4HSeO_4. $c_{\lambda\lambda}$ vs. T [90Zra]. $c_{\lambda\lambda}$: elastic stiffness constant at 10 MHz.

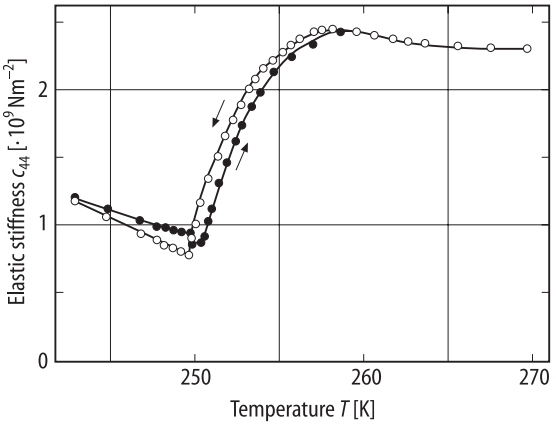

Fig. 40A-9-050. NH_4HSeO_4. c_{44} vs. T [90Zra]. f = 10 MHz.

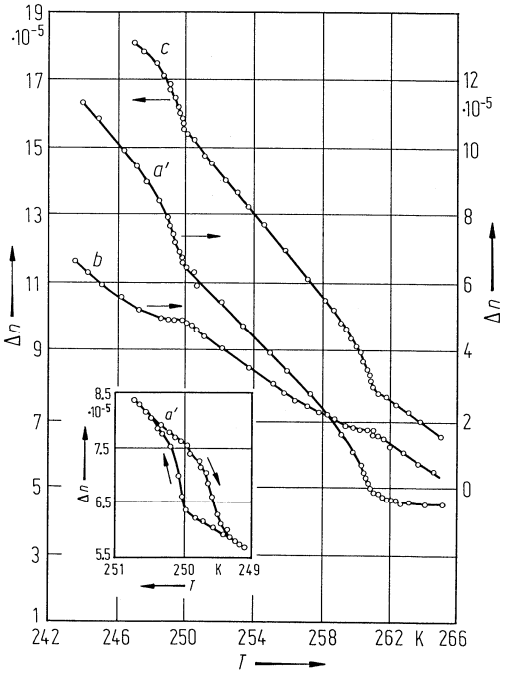

Fig. 40A-9-051. NH_4HSeO_4. Δn vs. T [82Mar]. $\lambda = 632.8$ nm. a', b and c denote birefringence for light propagating along the a' , b and c axes, respectively.

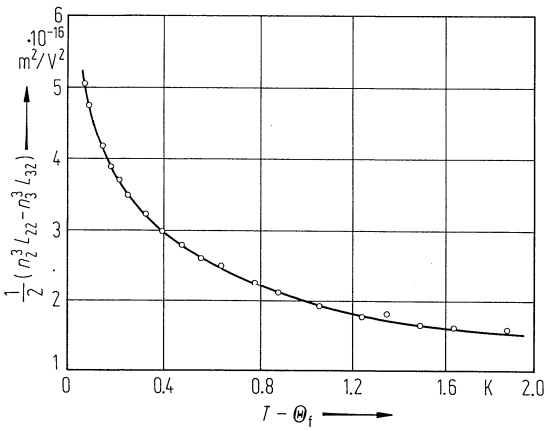

Fig. 40A-9-052. NH_4HSeO_4. $(n_2^3 L_{22} - n_3^3 L_{32})/2$ vs. $T - \Theta_f$ [82Mar]. L_{22}, L_{32}: quadratic electrooptic constant for $\lambda = 632.8$ nm.

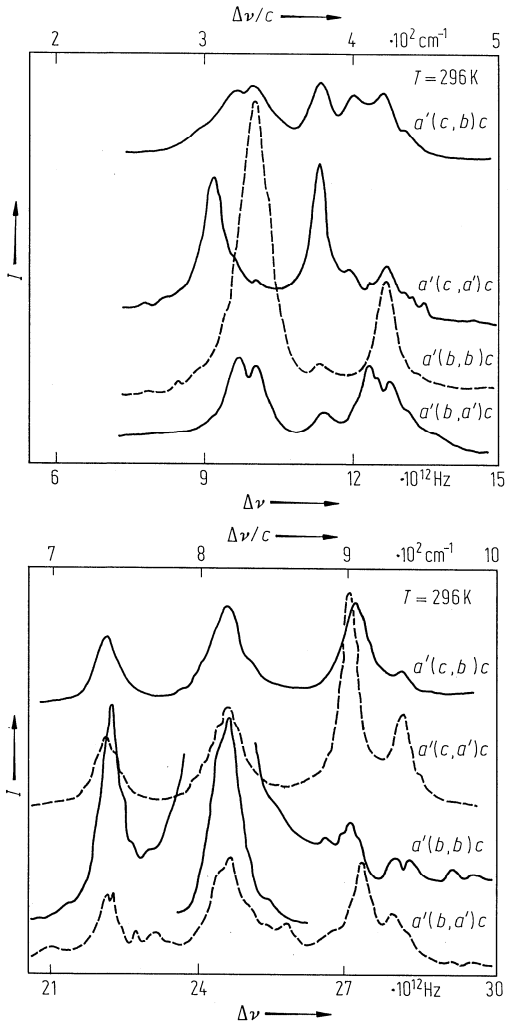

Fig. 40A-9-053. NH_4HSeO_4. I vs. $\Delta\nu$ [83Smo]. I: intensity of Raman scattering spectra. T = 296 K. Parameter: scattering geometry.

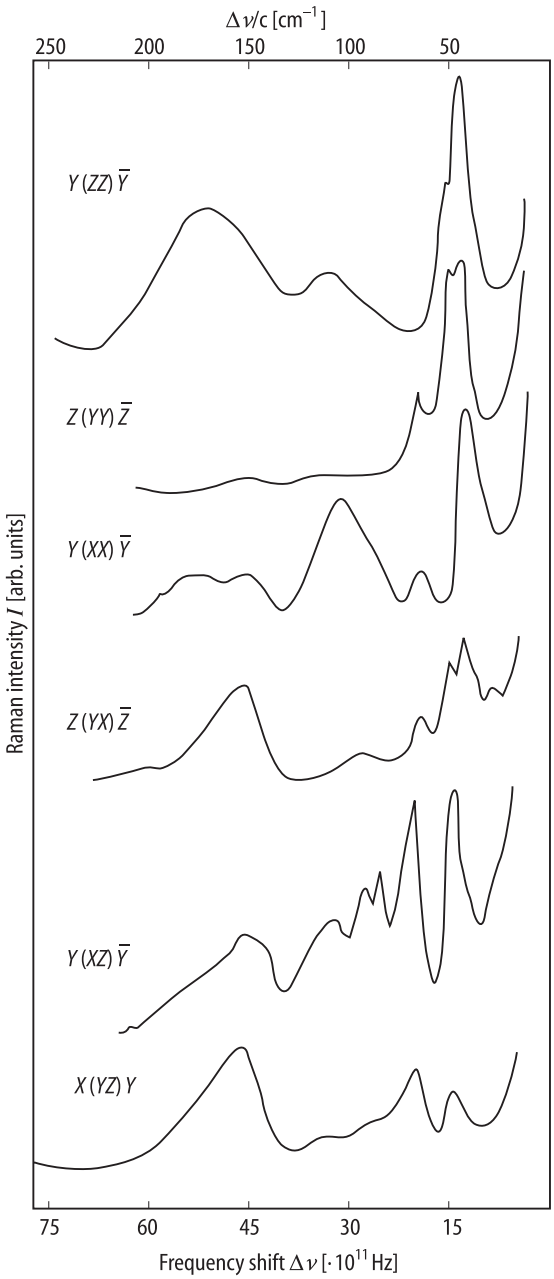

Fig. 40A-9-054. NH_4HSeO_4. I vs. $\Delta\nu$ [90Pas]. I: intensity of Raman scattering spectra. T = 295 K. Parameter: scattering geometry.

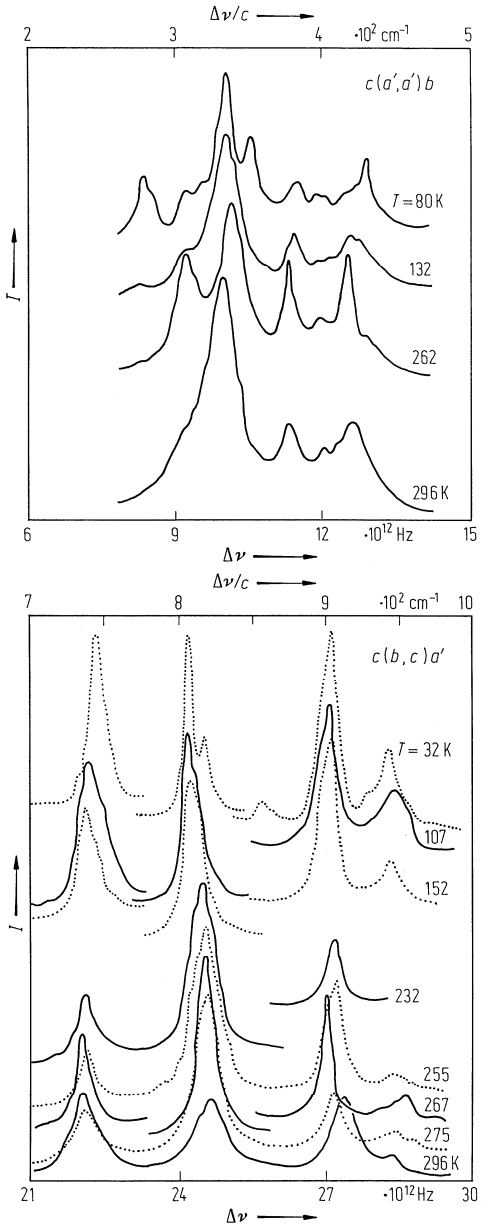

Fig. 40A-9-055. NH_4HSeO_4. I vs. $\Delta\nu$ [83Smo]. I: intensity of Raman scattering spectra. Parameter: T.

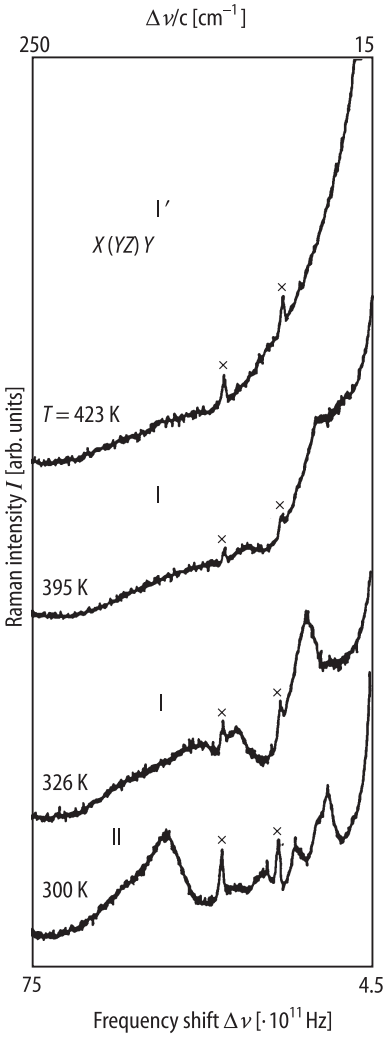

Fig. 40A-9-056. NH_4HSeO_4. I vs. $\Delta\nu$ [90Pas]. I: intensity of Raman scattering spectra. Parameter: T. Crosses denote the laser lines.

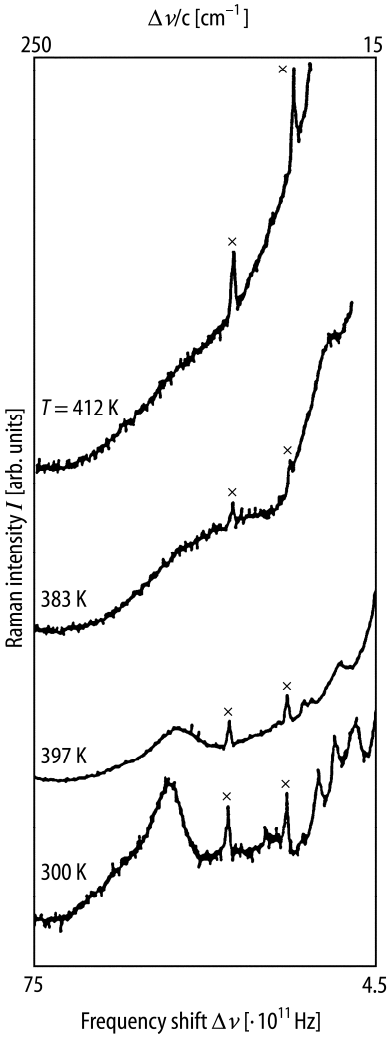

Fig. 40A-9-057. ND_4DSeO_4. I vs. $\Delta\nu$ [90Pas]. I: intensity of Raman scattering spectra. Parameter: T. Crosses denote the laser lines.

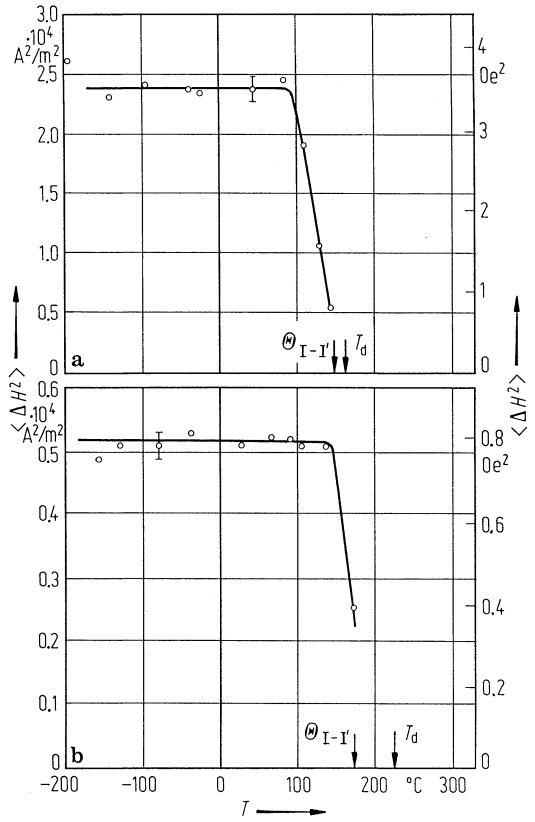

Fig. 40A-9-058. NH_4HSeO_4, $RbHSeO_4$. $<\Delta H^2>$ vs. T [84Mos]. $<\Delta H^2>$: second moment of proton NMR line of polycrystalline (**a**) NH_4HSeO_4 and (**b**) $RbHSeO_4$. T_d: decomposition temperature.

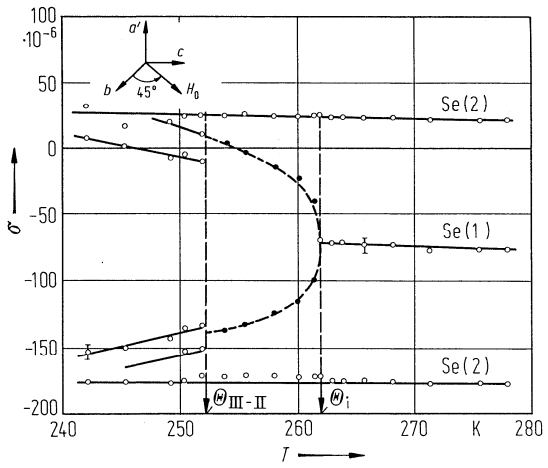

Fig. 40A-9-059. NH_4HSeO_4. ^{77}Se chemical shift vs. T [83Ale]. Open circle: positions of the spectral lines; full circle: positions of the edge singularities. Θ_i: temperature of incommensurate ordering of protons.

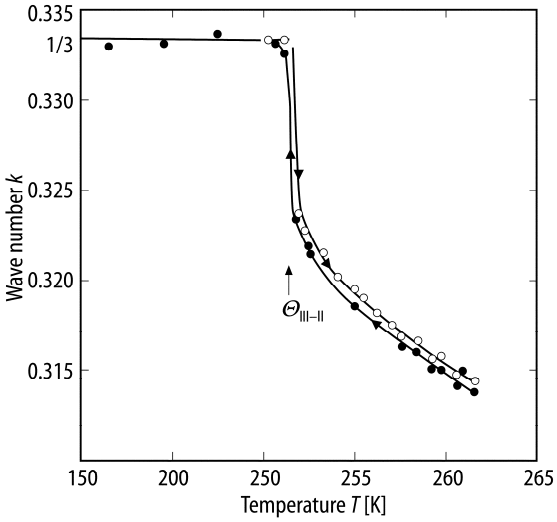

Fig. 40A-9-060. NH_4HSeO_4. k vs. T [89Den]. k: incommensurate wave vector in phase II. Cooling run (full circle), warming run (open circle).

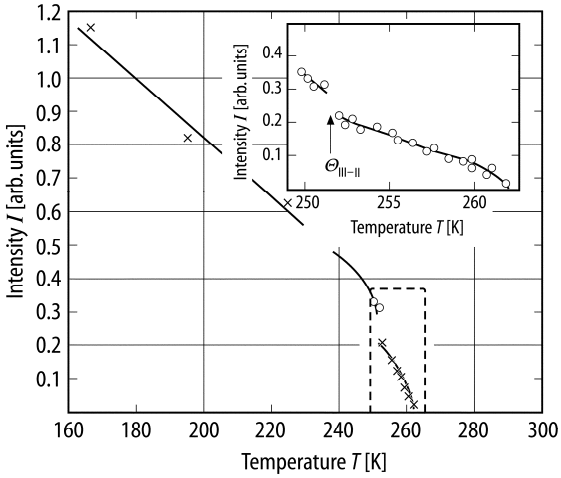

Fig. 40A-9-061. NH_4HSeO_4. I vs. T [89Den]. I: integrated intensity of (–2, 2, ±q) reflection of neutrons.

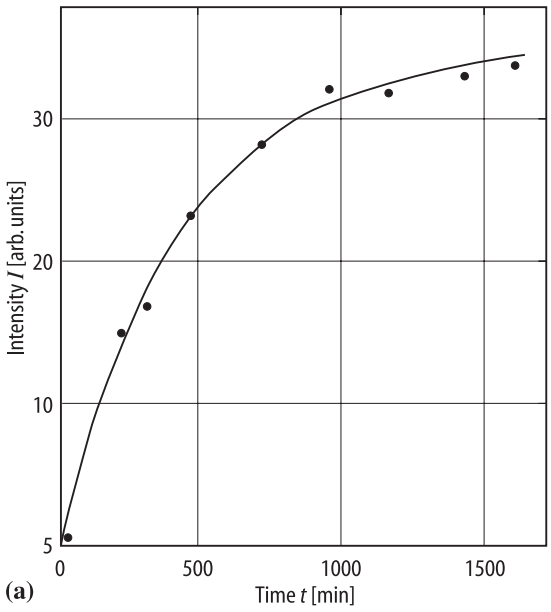

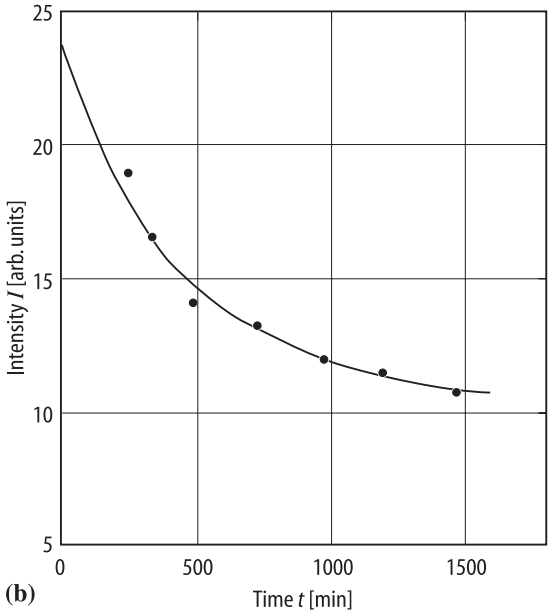

Fig. 40A-9-062. ND_4DSeO_4. I vs. t [89Den]. I: integrated intensity of neutrons. T = 307.1 K. (**a**) (0, 2, 1) reflection, (**b**) (–2, 2, ±1/2) reflection.